

Green's Function Extraction for Interfaces With Impedance Boundary Conditions

Evert Slob and Kees Wapenaar

Abstract—Theory and experiments to obtain the response between two receivers from cross correlations of wave fields recorded at these receivers are well established. The principle relies on mutually spatial and temporal uncorrelated contributions from sources on a boundary enclosing the two receivers, which upon cross correlation interfere only constructively for signals traveling between the two receivers. It has, therefore, become generally known as interferometry. The theory includes situations with flow, mechanical, and electromagnetic field fluctuations, and their mutual coupling. Here, we present an electromagnetic theory for Green's function retrieval from cross correlations that incorporates general bianisotropic media in which interfaces are present where bianisotropic impedance boundary conditions apply. The derived Green's function representation shows that in lossless media and for interfaces with lossless impedance boundary conditions the Green's function between two receivers is obtained by cross correlating the recordings of these receivers from sources on a boundary enclosing them. We show numerical examples in 2-D where proper solutions are numerically tractable and practical approximations illustrate that numerically less intensive algorithms lead to acceptable results and accurate extraction of reflections from impedance boundary surfaces. Because the method is data driven, it is suitable for experimental Green's function extraction from measured data.

Index Terms—Bianisotropic media, impedance boundary conditions, interferometry.

I. INTRODUCTION

INTERFEROMETRIC Green's function extraction involves cross correlation and integration of recorded fields. Here it is used to obtain the Green's function between two receivers from cross correlation of their recordings. The method of extracting the Green's function from cross correlating observations simultaneously made at two different locations can be envisaged as coherent interferometric radiometry. Presently known electromagnetic formulations rely on continuity conditions of the transverse electric and magnetic field components across finite jump discontinuities in medium parameter values [1]–[5].

The interaction of electromagnetic wave fields with interfaces across which the wave field components satisfy jump-average

conditions have been studied for a long time. In the earth sciences this was discussed for fields in the diffusive approximation, for a strongly conductive interface [6]. In the case of a conductive interface charges cannot be built up and the current that is generated at the interface gives rise to a jump in the tangential magnetic field components, linearly proportional to the tangential electric field components. The ratio of the electric field and the magnetic field jump is the specific boundary resistivity. Interface conditions of this type are known as impedance boundary conditions. Impedance boundary conditions are used for modern scattering computations of large and curved objects, and corrugated surfaces [7]–[13], of half planes [14], in biomedical engineering [15] and for bianisotropic impedance boundaries with jump conditions [16], [17].

In this work general linear electromagnetic media are incorporated, which are represented by a full constitutive matrix [18]. An early example is the dual polarized ring laser [19] that can be used in downhole formation testing in oil exploration. For bianisotropic media with continuity boundary conditions, for the transverse components of the electric and magnetic fields, the interferometric relations are derived in [20]. Bianisotropic media are of growing importance in the fabrication of metamaterials [21] that can be used for creating impedance boundary conditions [22], [23]. In this paper, the Green's function retrieval is formulated for interfaces with general linear impedance boundary conditions. General symmetry properties of the interface material parameter matrix is given for reciprocal and nonreciprocal lossless impedance boundary conditions that lead to Green's function extraction from contributions of sources located on a boundary. We show numerical examples in 2-D to illustrate the possibilities and restrictions.

II. RECIPROCITY

The theory is developed in six-vector notation [24] and three unitary six-matrices, \mathbf{K} , \mathbf{N} , \mathbf{J} , are introduced as

$$\mathbf{K} = \begin{pmatrix} -\mathbf{I} & \mathbf{O} \\ \mathbf{O} & \mathbf{I} \end{pmatrix}, \quad \mathbf{N} = \begin{pmatrix} \mathbf{O} & -\mathbf{I} \\ \mathbf{I} & \mathbf{O} \end{pmatrix} \quad (1)$$

while the matrix \mathbf{J} is obtained as $\mathbf{J} = \mathbf{K}\mathbf{N}$ and the unit matrix \mathbf{I} is used for the 3×3 and 6×6 unit matrices, but no confusion occurs. Note that $\mathbf{N}^T = \mathbf{N}^{-1} = -\mathbf{N}$, $\mathbf{K}^T = \mathbf{K} = \mathbf{K}^{-1}$ and $\mathbf{J}^T = \mathbf{J} = \mathbf{J}^{-1}$, which relations are used many times. The macroscopic space-time electromagnetic field is determined by the electric field $\mathbf{E}(\mathbf{x}, t)$, the magnetic field $\mathbf{H}(\mathbf{x}, t)$, the electric and magnetic flux densities $\mathbf{D}(\mathbf{x}, t)$, $\mathbf{B}(\mathbf{x}, t)$, and the external source volume densities of electric and magnetic currents, $\{\mathbf{J}^e(\mathbf{x}, t), \mathbf{J}^m(\mathbf{x}, t)\}$, respectively. The time-Fourier transform of a space-time dependent quantity is defined as $\hat{f}(\mathbf{x}, \omega) =$

Manuscript received March 02, 2011; manuscript revised July 21, 2011; accepted July 30, 2011. Date of publication September 15, 2011; date of current version January 05, 2012.

The authors are with the Department of Geotechnology, Delft University of Technology (TU Delft), Stevinweg 1, 2628 CN Delft, The Netherlands (e-mail: e.c.slob@tudelft.nl; c.p.a.wapenaar@tudelft.nl).

Color versions of one or more of the figures in this paper are available online at <http://ieeexplore.ieee.org>.

Digital Object Identifier 10.1109/TAP.2011.2167942

$\int \exp(-j\omega t) f(\mathbf{x}, t) dt$, where j is the imaginary unit and ω denotes angular frequency. The frequency domain constitutive relations are given by $\hat{\mathbf{D}} = \hat{\boldsymbol{\epsilon}}\hat{\mathbf{E}} + \hat{\boldsymbol{\xi}}\hat{\mathbf{H}}$ and $\hat{\mathbf{B}} = \hat{\boldsymbol{\zeta}}\hat{\mathbf{E}} + \hat{\boldsymbol{\mu}}\hat{\mathbf{H}}$ where electric permittivity and magnetic permeability tensors are given by $\hat{\boldsymbol{\epsilon}}$ and $\hat{\boldsymbol{\mu}}$, while $\hat{\boldsymbol{\xi}}$, $\hat{\boldsymbol{\zeta}}$ denote the magneto-electric tensors. The effects of moving media and all possible time-relaxation mechanisms are incorporated in the frequency dependent complex valued material tensors. Maxwell's equations read $\mathbf{D}_x \hat{\mathbf{u}} + j\omega \hat{\mathbf{M}} \hat{\mathbf{u}} = \hat{\mathbf{s}}$, where the field vector $\hat{\mathbf{u}}$ is given by $\hat{\mathbf{u}}^T(\mathbf{x}, \omega) = (\hat{\mathbf{E}}^T, \hat{\mathbf{H}}^T)$ and the superscript T denotes transposition, $\hat{\mathbf{s}}^T(\mathbf{x}, \omega) = -(\{\hat{\mathbf{J}}^e\}^T, \{\hat{\mathbf{J}}^m\}^T)$ is the source vector, while \mathbf{D}_x is the matrix of spatial differential operators given by

$$\mathbf{D}_x = \begin{pmatrix} \mathbf{O} & \mathbf{D}_0^T \\ \mathbf{D}_0 & \mathbf{O} \end{pmatrix}, \quad \mathbf{D}_0 = \begin{pmatrix} 0 & -\partial_3 & \partial_2 \\ \partial_3 & 0 & -\partial_1 \\ -\partial_2 & \partial_1 & 0 \end{pmatrix}. \quad (2)$$

The material matrix is defined as

$$\hat{\mathbf{M}} = \begin{pmatrix} \hat{\boldsymbol{\epsilon}} & \hat{\boldsymbol{\xi}} \\ \hat{\boldsymbol{\zeta}} & \hat{\boldsymbol{\mu}} \end{pmatrix}. \quad (3)$$

We have the following symmetry property for the derivative matrix, $\mathbf{K} \mathbf{D}_x \mathbf{K} = -\mathbf{D}_x = -\mathbf{D}_x^T$.

Macroscopic impedance and admittance boundary conditions define linear relations between the electric and magnetic field components tangential to an interface [17]. General jump-average conditions are adopted in the frequency domain [25]

$$[\mathbf{N}_1 \hat{\mathbf{u}}] = -j\omega \hat{\mathbf{Y}} (\mathbf{N}_1 \hat{\mathbf{u}}) \quad (4)$$

with

$$\mathbf{N}_1 = \begin{pmatrix} \mathbf{N}_0 \mathbf{N}_0^T & \mathbf{O} \\ \mathbf{O} & \mathbf{N}_0^T \end{pmatrix}, \quad \hat{\mathbf{Y}} = \begin{pmatrix} \hat{\boldsymbol{\zeta}}^b & \hat{\boldsymbol{\mu}}^b \\ \hat{\boldsymbol{\epsilon}}^b & \hat{\boldsymbol{\xi}}^b \end{pmatrix} \quad (5)$$

with \mathbf{N}_0 defined as \mathbf{D}_0 but with the components of the spatial derivative, ∂_i , replaced by the components of the unit vector normal to the interface, n_i , $i = 1, 2, 3$. This formulation allows for approximations of thin high contrast layers [6], but they are exact for interfaces with perfect conductors, either electric, magnetic or electromagnetic [23] and generalized soft-and-hard (SHS) layers [22] or other conceivable interfaces with impedance boundary conditions (IBC) [26]. The jump and average across the interface are represented by $[\cdot]$, $\langle \cdot \rangle$, respectively; hence

$$[\hat{\mathbf{u}}(\mathbf{x}, \omega)] = \lim_{h \downarrow 0} (\hat{\mathbf{u}}(\mathbf{x} + h\mathbf{n}, \omega) - \hat{\mathbf{u}}(\mathbf{x} - h\mathbf{n}, \omega)) \quad (6)$$

$$\langle \hat{\mathbf{u}}(\mathbf{x}, \omega) \rangle = \lim_{h \downarrow 0} (\hat{\mathbf{u}}(\mathbf{x} + h\mathbf{n}, \omega) + \hat{\mathbf{u}}(\mathbf{x} - h\mathbf{n}, \omega)) / 2 \quad (7)$$

where \mathbf{x} is chosen at the interface. The interface permittivity and permeability are $\hat{\boldsymbol{\epsilon}}^b = \hat{\boldsymbol{\epsilon}}^b(\mathbf{x}, \mathbf{n}, \omega)$ and $\hat{\boldsymbol{\mu}}^b = \hat{\boldsymbol{\mu}}^b(\mathbf{x}, \mathbf{n}, \omega)$, while the magneto-electric interface parameter tensors are given by $\hat{\boldsymbol{\xi}}^b = \hat{\boldsymbol{\xi}}^b(\mathbf{x}, \mathbf{n}, \omega)$ and $\hat{\boldsymbol{\zeta}}^b = \hat{\boldsymbol{\zeta}}^b(\mathbf{x}, \mathbf{n}, \omega)$. First, the fields at both sides of the interface are separated to avoid sign problems with the matrices containing unit vectors normal to the interface. Let the two sides of the interface be denoted 1 and 2 and we use \mathbf{N}_1 to represent the unit vector, \mathbf{n}_1 normal to the interface, see Fig. 1,

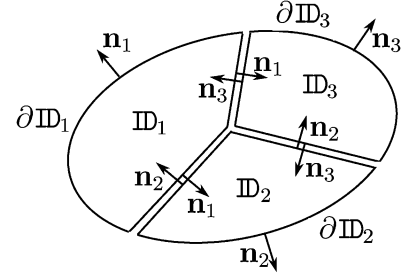


Fig. 1. Configuration for the reciprocity theorem internal interfaces with impedance boundary conditions.

such that $[\mathbf{N}_1 \hat{\mathbf{u}}] = \mathbf{N}_1 (\hat{\mathbf{u}}_2 - \hat{\mathbf{u}}_1)$ and then (4) can be written as $\mathbf{N}_1 \hat{\mathbf{u}}_2 = \hat{\mathbf{Z}} \mathbf{N}_1 \hat{\mathbf{u}}_1$, with $\hat{\mathbf{Z}} = (\mathbf{I} + j\omega \hat{\mathbf{Y}}/2)^{-1} (\mathbf{I} - j\omega \hat{\mathbf{Y}}/2)$.

A reciprocity theorem relates two states, labeled A and B , that can be nonidentical everywhere. Reciprocity of the time-convolution type is applied to a bounded spatial domain \mathbb{D} , and outer boundary $\partial \mathbb{D}$ with outward pointing unit normal vector $\mathbf{n}^T = \{n_1, n_2, n_3\}$, and internal interfaces Σ_{int} , where the boundary conditions of (4) apply, see Fig. 1. With the above definitions, the theorem reads [25]

$$\begin{aligned} & \int_{\mathbb{D}} [\hat{\mathbf{u}}_A^T \mathbf{K} \hat{\mathbf{s}}_B - \hat{\mathbf{s}}_A^T \mathbf{K} \hat{\mathbf{u}}_B] d^3 \mathbf{x} \\ &= \oint_{\partial \mathbb{D}} \hat{\mathbf{u}}_A^T \mathbf{K} \mathbf{N}_x \hat{\mathbf{u}}_B d^2 \mathbf{x} \\ &+ j\omega \int_{\mathbb{D}} [\hat{\mathbf{u}}_A^T (\mathbf{K} \hat{\mathbf{M}}_B - \hat{\mathbf{M}}_A^T \mathbf{K}) \hat{\mathbf{u}}_B] d^3 \mathbf{x} \\ &+ \int_{\Sigma_{\text{int}}} \hat{\mathbf{u}}_A^T \mathbf{N}_1^T (\mathbf{N} - \hat{\mathbf{Z}}_A^T \mathbf{N} \hat{\mathbf{Z}}_B) \mathbf{N}_1 \hat{\mathbf{u}}_B d^2 \mathbf{x} \quad (8) \end{aligned}$$

where \mathbf{N}_x is defined similar to \mathbf{D}_x , but with \mathbf{D}_0 replaced by \mathbf{N}_0 , and $\mathbf{K} \mathbf{N}_x \mathbf{K} = -\mathbf{N}_x = -\mathbf{N}_x^T$, and $\mathbf{K} \mathbf{N}_x = \mathbf{N}_1^T \mathbf{N} \mathbf{N}_1$ has been used. Note that for the integral over the nonperfect interfaces the fields $\hat{\mathbf{u}}_A$ and $\hat{\mathbf{u}}_B$, and the matrix \mathbf{N}_1 are all located on the “1-side”. Equation (8) is the general representation for two independent electromagnetic states in bianisotropic media. The sources and source locations as well as the media in the two states can be completely different. The first integral in the right-hand side of (8) represents the boundary integral over the outer boundary, where continuity conditions apply. The third integral in the right-hand side of (8) represents the boundary integral over all internal interfaces, where the impedance boundary conditions of (4) apply. This integral vanishes when $\hat{\mathbf{Z}}_A^T \mathbf{N} = \mathbf{N} \hat{\mathbf{Z}}_B^{-1}$ and interfaces satisfying these conditions are each other's adjoint. The adjoint of an interface impedance is denoted as $\hat{\mathbf{Z}}^{(a)}$ and it is related to the interface impedance through $\hat{\mathbf{Z}}^{(a)} = \mathbf{N}^T (\hat{\mathbf{Z}}^T)^{-1} \mathbf{N}$. This implies that the adjoint of the interface parameter matrix $\hat{\mathbf{Y}}^{(a)}$ is given by $\hat{\mathbf{Y}}^{(a)} = \mathbf{N} \hat{\mathbf{Y}}^T \mathbf{N}$, and

$$\hat{\mathbf{Y}}^{(a)} = \begin{pmatrix} -\hat{\boldsymbol{\xi}}^b & \hat{\boldsymbol{\epsilon}}^b \\ \hat{\boldsymbol{\mu}}^b & -\hat{\boldsymbol{\zeta}}^b \end{pmatrix}^T. \quad (9)$$

When these conditions hold for one and the same interface, it is called a self-adjoint, or reciprocal, interface and we have $\hat{\mathbf{Z}}^T \mathbf{N} = \mathbf{N} \hat{\mathbf{Z}}^{-1}$ and $\hat{\mathbf{Y}}^T \mathbf{N} = \mathbf{N}^T \hat{\mathbf{Y}}$.

The volume integral in the right-hand side of (8) vanishes when $\hat{\mathbf{M}}_A = \mathbf{K} \hat{\mathbf{M}}_B^T \mathbf{K}$, which implies that $\hat{\mathbf{e}}_A = \hat{\mathbf{e}}_B^T$, $\hat{\boldsymbol{\mu}}_A = \hat{\boldsymbol{\mu}}_B^T$, $\hat{\boldsymbol{\zeta}}_A = -\hat{\boldsymbol{\xi}}_B^T$ and $\hat{\boldsymbol{\xi}}_A = -\hat{\boldsymbol{\zeta}}_B^T$. This situation is discussed in [20] and here only the necessary results are used. The adjoint medium is denoted $\hat{\mathbf{M}}^{(a)}$ and its relation to the material matrix is given by $\hat{\mathbf{M}}^{(a)} = \mathbf{K} \hat{\mathbf{M}}^T \mathbf{K}$. If these conditions hold in one and the same medium, the medium is called self-adjoint or reciprocal and we have $\hat{\mathbf{M}} = \mathbf{K} \hat{\mathbf{M}}^T \mathbf{K}$.

A. Source-Receiver Reciprocity

The Green's function expression of source-receiver reciprocity is obtained by taking state B as the adjoint of state A, and hence the second and third integrals in the right-hand side of (8) vanish. The material matrices are given by $\hat{\mathbf{M}}_A = \hat{\mathbf{M}}$ and $\hat{\mathbf{M}}_B = \hat{\mathbf{M}}^{(a)}$, while the interface impedance matrices are $\hat{\mathbf{Z}}_A = \hat{\mathbf{Z}}$ and $\hat{\mathbf{Z}}_B = \hat{\mathbf{Z}}^{(a)}$. The 6×1 source vectors $\hat{\mathbf{s}}_{A,B}(\mathbf{x}, \omega)$ are replaced by the 6×6 unit strength point source matrices $\mathbf{I} \delta(\mathbf{x} - \mathbf{x}_{A,B})$, where \mathbf{I} is the identity matrix. The field vector $\hat{\mathbf{u}}_A(\mathbf{x}, \omega)$ is correspondingly replaced by the 6×6 Green's matrix $\hat{\mathbf{G}}(\mathbf{x}, \mathbf{x}_A, \omega)$, while the field vector $\hat{\mathbf{u}}_B$ is replaced by the adjoint Green's matrix $\hat{\mathbf{G}}^{(a)}(\mathbf{x}, \mathbf{x}_B, \omega)$. In the Green's matrix each column represents the Green's functions for all the electric and magnetic field components for a single source type and direction, while each row represents a single field type and component for all source types and directions. If we take \mathbf{x}_A and \mathbf{x}_B inside \mathbb{D} and assume that outside some sphere with finite radius the medium is isotropic and homogeneous, then the boundary integral also vanishes, leaving the source-receiver reciprocity relation as

$$\mathbf{K} \hat{\mathbf{G}}^T(\mathbf{x}_B, \mathbf{x}_A, \omega) \mathbf{K} = \hat{\mathbf{G}}^{(a)}(\mathbf{x}_A, \mathbf{x}_B, \omega) \quad (10)$$

which expresses the equality of a measurement in a certain medium to an other measurement in an adjoint medium, with interchanged source and receiver type, vector component and location. The matrix \mathbf{K} accounts for possible sign changes upon interchanging source and receiver.

III. POWER BALANCE

The here derived interferometric relation originates in the correlation-type reciprocity theorem, which reads [27]–[29]

$$\begin{aligned} & \int_{\mathbb{D}} [\hat{\mathbf{u}}_A^\dagger \hat{\mathbf{s}}_B + \hat{\mathbf{s}}_A^\dagger \hat{\mathbf{u}}_B] d^3 \mathbf{x} \\ &= \oint_{\partial \mathbb{D}} \hat{\mathbf{u}}_A^\dagger \mathbf{N}_x \hat{\mathbf{u}}_B d^2 \mathbf{x} \\ & \quad - j\omega \int_{\mathbb{D}} \hat{\mathbf{u}}_A^\dagger (\hat{\mathbf{M}}_A^\dagger - \hat{\mathbf{M}}_B) \hat{\mathbf{u}}_B d^3 \mathbf{x} \\ & \quad + \int_{\Sigma_{\text{int}}} \hat{\mathbf{u}}_A^\dagger \mathbf{N}_1^\dagger (\mathbf{J} - \hat{\mathbf{Z}}_A^\dagger \mathbf{J} \hat{\mathbf{Z}}_B) \mathbf{N}_1 \hat{\mathbf{u}}_B d^2 \mathbf{x} \quad (11) \end{aligned}$$

where $\mathbf{N}_x = \mathbf{N}_1^\dagger \mathbf{J} \mathbf{N}_1$ has been used and the superscript \dagger denotes matrix transposition and complex conjugation. If in (11) $\mathbf{J} \hat{\mathbf{Z}}_A^\dagger \mathbf{J} = \hat{\mathbf{Z}}_B^{-1}$ the interface is lossless, which can occur either when the interfaces in both states are lossless or when the interface in one state dissipates energy from the field and in the other state it delivers the same amount of energy to the field in which case $\hat{\mathbf{Y}}_A^\dagger = \mathbf{J} \hat{\mathbf{Y}}_B \mathbf{J}$. Then it is found that $(\hat{\boldsymbol{\xi}}_A^b)^\dagger = \hat{\boldsymbol{\xi}}_B^b$, $(\hat{\boldsymbol{\mu}}_A^b)^\dagger = \hat{\boldsymbol{\mu}}_B^b$ and $(\hat{\boldsymbol{\zeta}}_A^b)^\dagger = \hat{\boldsymbol{\xi}}_B^b$, $(\hat{\boldsymbol{\xi}}_A^b)^\dagger = \hat{\boldsymbol{\zeta}}_B^b$. The parameter matrix of the adjoint interface is related to that of the interface as

$$\mathbf{J} \hat{\mathbf{Z}}^\dagger \mathbf{J} = \mathbf{K} \left(\hat{\mathbf{Z}}^{(a)*} \right)^{-1} \mathbf{K} \quad (12)$$

$$\mathbf{J} \hat{\mathbf{Y}}^\dagger \mathbf{J} = -\mathbf{K} \hat{\mathbf{Y}}^{(a)*} \mathbf{K} = \begin{pmatrix} \hat{\boldsymbol{\xi}}^b & \hat{\boldsymbol{\xi}}^b \\ \hat{\boldsymbol{\mu}}^b & \hat{\boldsymbol{\zeta}}^b \end{pmatrix}^\dagger \quad (13)$$

where the superscript $*$ denotes complex conjugation.

When $\mathbf{J} \hat{\mathbf{Y}} \mathbf{J} = \hat{\mathbf{Y}}^\dagger$, the interface is lossless, but not necessarily reciprocal. The medium is lossless when $\hat{\mathbf{M}}^\dagger = \hat{\mathbf{M}}$. When states A and B are the same, and both the interface and the medium are lossless the last two integrals of (11) vanish.

A. Correlation Type Green's Matrix Representation

Equation (11) is used to derive a representation of the Green's matrix in terms of cross correlations. Point source matrices and Green's matrices replace the source and field vectors. The points \mathbf{x}_A and \mathbf{x}_B are chosen in \mathbb{D} and both states have the same interface and medium parameters $\hat{\mathbf{Z}}_A = \hat{\mathbf{Z}}_B = \hat{\mathbf{Z}}$ and $\hat{\mathbf{M}}_A = \hat{\mathbf{M}}_B = \hat{\mathbf{M}}$. With these choices the correlation type Green's matrix representation is given by

$$\begin{aligned} & \hat{\mathbf{G}}^\dagger(\mathbf{x}_B, \mathbf{x}_A, \omega) + \hat{\mathbf{G}}(\mathbf{x}_A, \mathbf{x}_B, \omega) \\ &= \oint_{\partial \mathbb{D}} \hat{\mathbf{G}}^\dagger(\mathbf{x}, \mathbf{x}_A, \omega) \mathbf{N}_x \hat{\mathbf{G}}(\mathbf{x}, \mathbf{x}_B, \omega) d^2 \mathbf{x} \\ & \quad + \int_{\mathbb{D}} \hat{\mathbf{G}}^\dagger(\mathbf{x}, \mathbf{x}_A, \omega) \Delta \hat{\mathbf{M}} \hat{\mathbf{G}}(\mathbf{x}, \mathbf{x}_B, \omega) d^3 \mathbf{x} \\ & \quad + \int_{\Sigma_{\text{int}}} \hat{\mathbf{G}}^\dagger(\mathbf{x}, \mathbf{x}_A, \omega) \Delta \hat{\mathbf{M}}^b \hat{\mathbf{G}}(\mathbf{x}, \mathbf{x}_B, \omega) d^3 \mathbf{x} \quad (14) \end{aligned}$$

where the contrast functions are both Hermitian and given by

$$\Delta \hat{\mathbf{M}} = j\omega (\hat{\mathbf{M}} - \hat{\mathbf{M}}^\dagger) \quad (15)$$

$$\Delta \hat{\mathbf{M}}^b = \mathbf{N}_1^T [\mathbf{J} - \hat{\mathbf{Z}}^\dagger \mathbf{J} \hat{\mathbf{Z}}] \mathbf{N}_1. \quad (16)$$

It is noted that now both states exist in one and the same medium. Furthermore, these states can occur simultaneously, but that is not mandatory. No assumptions have been made about the internal interfaces and material matrices, $\hat{\mathbf{Z}}$ and $\hat{\mathbf{M}}$. Obviously, at each interface where $\hat{\mathbf{Z}}^\dagger \mathbf{J} = \mathbf{J} \hat{\mathbf{Z}}^{-1}$, the interface is lossless and the third integral in the right-hand side of (14) vanishes. Only the anti-Hermitian part of $\hat{\mathbf{M}}$ remains in the representation, which is the part accounting for energy dissipation. Equation (14) is a general representation of the electromagnetic Green's matrix for arbitrary bianisotropic media, including arbitrary IBC interfaces. Equation (14) represents the Green's

functions between \mathbf{x}_A and \mathbf{x}_B obtained from integral contributions of received Green's functions at the boundary $\partial\mathbb{D}$, at the internal interfaces Σ_{int} and in the volume \mathbb{D} , in a heterogeneous bianisotropic medium with piecewise continuous interfaces.

IV. GREEN'S FUNCTION RETRIEVAL

Equation (11) is used to derive an interferometric representation of the Green's matrix in terms of cross correlations. The points \mathbf{x}_A and \mathbf{x}_B are chosen in \mathbb{D} , but the adjoint states are taken for both A and B , hence again both states occur in one and the same medium but now with $\hat{\mathbf{Z}}_A = \hat{\mathbf{Z}}_B = \hat{\mathbf{Z}}^{(a)}$ and $\hat{\mathbf{M}}_A = \hat{\mathbf{M}}_B = \hat{\mathbf{M}}^{(a)}$. Point source matrices are used and, as a consequence of the medium and interface impedance parameters, adjoint Green's matrices replace the source and field vectors. Equation (10) is used together with the symmetry relations for \mathbf{N}_x , and \mathbf{N}_1 , and for $\hat{\mathbf{Z}}^{(a)}$ and $\hat{\mathbf{M}}^{(a)}$. Transposing both sides of the resulting equation yields

$$\begin{aligned} & \hat{\mathbf{G}}(\mathbf{x}_B, \mathbf{x}_A, \omega) + \hat{\mathbf{G}}^\dagger(\mathbf{x}_A, \mathbf{x}_B, \omega) \\ &= - \oint_{\partial\mathbb{D}} \hat{\mathbf{G}}(\mathbf{x}_B, \mathbf{x}, \omega) \mathbf{N}_x \hat{\mathbf{G}}^\dagger(\mathbf{x}_A, \mathbf{x}, \omega) d^2\mathbf{x} \\ & \quad + \int_{\mathbb{D}} \hat{\mathbf{G}}(\mathbf{x}_B, \mathbf{x}, \omega) \Delta\hat{\mathbf{M}} \hat{\mathbf{G}}^\dagger(\mathbf{x}_A, \mathbf{x}, \omega) d^3\mathbf{x} \\ & \quad + \int_{\Sigma_{\text{int}}} \hat{\mathbf{G}}(\mathbf{x}_B, \mathbf{x}, \omega) \Delta\hat{\mathbf{M}}^b \hat{\mathbf{G}}^\dagger(\mathbf{x}_A, \mathbf{x}, \omega) d^2\mathbf{x} \end{aligned} \quad (17)$$

where the contrast function $\Delta\hat{\mathbf{M}}$ is the same as in (16), while the impedance boundary contrast matrix is now given by

$$\Delta\hat{\mathbf{M}}^b = -\mathbf{N}_1^T \mathbf{J} \left[\mathbf{J} - (\hat{\mathbf{Z}}^\dagger \mathbf{J} \hat{\mathbf{Z}})^{-1} \right] \mathbf{J} \mathbf{N}_1. \quad (18)$$

No assumptions have been made about the internal interfaces and material matrices, $\hat{\mathbf{Z}}$ and $\hat{\mathbf{M}}$, other than that their adjoint exist. Equation (17) is a general representation of the electromagnetic Green's matrix, between \mathbf{x}_A and \mathbf{x}_B located in the same medium, obtained from integral contributions from sources at the boundary, $\partial\mathbb{D}$, at the internal generalized impedance interfaces, Σ_{int} , and inside the volume, \mathbb{D} , in an arbitrary heterogeneous bianisotropic medium, with IBC interfaces. It is valid for reciprocal and nonreciprocal IBC interfaces and media. When the media and IBC interfaces dissipate no energy, the full Green's matrix can be obtained from sources on the boundary only. Hence, even for an arbitrary heterogeneous bianisotropic medium with IBC interfaces, absence of energy dissipation is a sufficient condition for obtaining the Green's function from the cross correlation of two recordings from sources on a closed boundary only. In the time domain the Green's matrix is causal; hence, $\mathbf{G}(\mathbf{x}_B, \mathbf{x}_A, t) = \mathbf{0}$ for $t < 0$, and the time reversed Green's function is time reversed causal; hence, $\mathbf{G}^T(\mathbf{x}_A, \mathbf{x}_B, -t) = \mathbf{0}$ for $t > 0$. For this reason $\mathbf{G}(\mathbf{x}_B, \mathbf{x}_A, t)$ or $\mathbf{G}^T(\mathbf{x}_A, \mathbf{x}_B, -t)$ can be easily retrieved from the left-hand side of (17), $\mathbf{G}(\mathbf{x}_B, \mathbf{x}_A, t) + \mathbf{G}^T(\mathbf{x}_A, \mathbf{x}_B, -t)$, by taking the causal or time-reversed causal part, respectively. In general, the application of (17) requires independent measurements of sources at all points in the domain and at the

boundary of \mathbb{D} . In applications of remote sensing without a source, the most interesting situation is the lossless variant with $\hat{\mathbf{Y}} = \mathbf{J} \hat{\mathbf{Y}}^\dagger \mathbf{J}$, where the interfaces can be dispersive, but dissipate no energy, and with similar medium properties $\hat{\mathbf{M}} = \hat{\mathbf{M}}^\dagger$.

A. Lossless Interfaces

For lossless interfaces and media the matrices satisfy $\mathbf{J} \hat{\mathbf{Y}} \mathbf{J} = \hat{\mathbf{Y}}^\dagger$ and $\hat{\mathbf{M}} = \hat{\mathbf{M}}^\dagger$, leading to $\Delta\hat{\mathbf{M}}^b = \mathbf{0}$ and $\Delta\hat{\mathbf{M}} = \mathbf{0}$. Note that this occurs when $\hat{\boldsymbol{\epsilon}}^b = (\hat{\boldsymbol{\epsilon}}^b)^\dagger$, $\hat{\boldsymbol{\mu}}^b = (\hat{\boldsymbol{\mu}}^b)^\dagger$ and $\hat{\boldsymbol{\xi}}^b = (\hat{\boldsymbol{\zeta}}^b)^\dagger$ for the interface parameter matrices and the same conditions apply for the material parameter matrices. These choices allow for nonreciprocal media and impedance interfaces. Then (17) directly reduces to

$$\begin{aligned} & \hat{\mathbf{G}}(\mathbf{x}_B, \mathbf{x}_A, \omega) + \hat{\mathbf{G}}^\dagger(\mathbf{x}_A, \mathbf{x}_B, \omega) \\ &= - \oint_{\partial\mathbb{D}} \hat{\mathbf{G}}(\mathbf{x}_B, \mathbf{x}, \omega) \mathbf{N}_x \hat{\mathbf{G}}^\dagger(\mathbf{x}_A, \mathbf{x}, \omega) d^2\mathbf{x}. \end{aligned} \quad (19)$$

For lossless IBC interfaces in lossless media the Green's matrix between \mathbf{x}_A and \mathbf{x}_B is obtained from cross correlations of recordings from responses to independent impulsive sources on $\partial\mathbb{D}$ only. When the data, generated by one of the sources at the boundary and recorded by two receivers, are cross correlated with each other and summed over all the source contributions at the boundary, the result is a pulse echo experiment with one of the receivers acting as a source and in absence of the original sources at the boundary, as sketched in Fig. 2. To make (19) suited for uncorrelated noise sources, \mathbf{N}_x must be diagonalized. This involves the separation of contributions from the sources for inward and outward traveling waves and the procedure is outlined in [28]. A suitable diagonalization procedure is available when the noise sources lie on a boundary in a lossless isotropic medium [30]. Then, e.g., the electric subset of (19) is in the time domain given by

$$\begin{aligned} & \left\{ \mathbf{G}^{ee}(\mathbf{x}_B, \mathbf{x}_A, t) + [\mathbf{G}^{ee}(\mathbf{x}_A, \mathbf{x}_B, -t)]^T \right\} * C(t) \\ & \propto \left\langle \mathbf{E}^{\text{obs}}(\mathbf{x}_B, t) * \left\{ \mathbf{E}^{\text{obs}}(\mathbf{x}_A, -t) \right\}^T \right\rangle \end{aligned} \quad (20)$$

where $C(t)$ denotes the autocorrelation of the noise sources and $\langle \cdot \rangle$ denotes a spatial ensemble average. This expression is similar to the results obtained for anisotropic and bianisotropic media [3], [20]. In (20) time convolution is indicated by $*$, the Green's function corresponding to the electric field generated by an electric current source is represented by \mathbf{G}^{ee} , while \mathbf{E}^{obs} denotes the observed electric field vector due to uncorrelated noise sources. For random white noise sources, $C(t) = \delta(t)$ and the Green's function is retrieved.

V. ELECTRIC FIELD GREEN'S FUNCTION RETRIEVAL

We now reduce (17) to retrieve the Green's function for the electric field generated by an electric current source. We first write the interface impedance matrix as

$$\hat{\mathbf{Z}} = \begin{pmatrix} Z_{kr}^{(11)} & Z_{kr}^{(12)} \\ Z_{kr}^{(21)} & Z_{kr}^{(22)} \end{pmatrix} \quad (21)$$

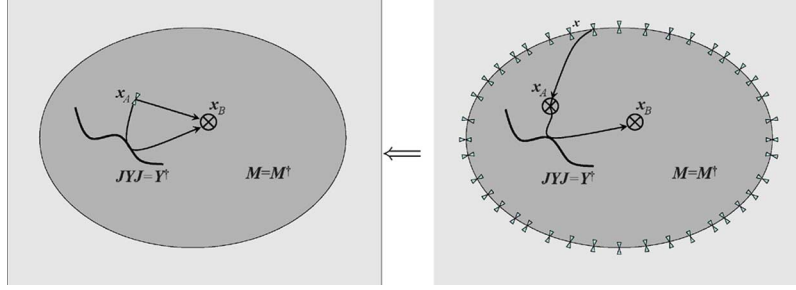


Fig. 2. Right graph depicts the situation for one source; when the data recorded at \mathbf{x}_A and \mathbf{x}_B is cross correlated for each source at the boundary and summed over all sources as expressed in the right-hand side of equation (19), the result is an experiment in absence of sources at the boundary, but where one of the original receivers acts as a source as depicted in the left graph as an illustration of the first Green's function in the left-hand side of equation (19).

where the subscripts kr denote the Cartesian tensor components of each sub-matrix $\hat{\mathbf{Z}}^{(\alpha\beta)}$ for $\alpha = (1, 2)$ and $\beta = (1, 2)$. The matrix for the impedance condition is

$$\mathbf{J} - \hat{\mathbf{Z}}_A^\dagger \mathbf{J} \hat{\mathbf{Z}}_B = \begin{pmatrix} b_{ik}^{(11)} & b_{ik}^{(12)} \\ b_{ik}^{(21)} & b_{ik}^{(22)} \end{pmatrix} \quad (22)$$

with the sub-matrices given by

$$b_{ik}^{(11)} = - \left(Z_{ji;A}^{(11)} \right)^* Z_{jk;B}^{(21)} - \left(Z_{ji;A}^{(21)} \right)^* Z_{jk;B}^{(11)} \quad (23)$$

$$b_{ik}^{(12)} = \delta_{ik} - \left(Z_{ji;A}^{(11)} \right)^* Z_{jk;B}^{(22)} - \left(Z_{ji;A}^{(21)} \right)^* Z_{jk;B}^{(12)} \quad (24)$$

$$b_{ik}^{(21)} = \delta_{ik} - \left(Z_{ji;A}^{(22)} \right)^* Z_{jk;B}^{(11)} - \left(Z_{ji;A}^{(12)} \right)^* Z_{jk;B}^{(21)} \quad (25)$$

$$b_{ik}^{(22)} = - \left(Z_{ji;A}^{(12)} \right)^* Z_{jk;B}^{(22)} - \left(Z_{ji;A}^{(22)} \right)^* Z_{jk;B}^{(12)}. \quad (26)$$

We also introduce two new directional tensors $L_{ik} = \epsilon_{ijk} n_j$, where L_{ik} is equal to \mathbf{N}_0 in subscript notation, and $\tau_{im} = L_{ik} L_{km}$, being equal to $\mathbf{N}_0 \mathbf{N}_0^T$ in subscript notation, and $\epsilon_{ijk} = (i-j)(j-k)(k-i)/2$. These newly introduced tensors are used in (11) to write it out in Cartesian tensor components for the electric field. We keep electric current sources in both states, but take the magnetic current sources to be zero $\hat{\mathbf{J}}_{p;A}^m = 0$ and $\hat{\mathbf{J}}_{p;B}^m = 0$. For a lossless medium with interfaces satisfying impedance boundary conditions, we find

$$\begin{aligned} & \int_{\mathbf{x} \in \mathbb{D}} \left[\hat{\mathbf{E}}_{k;A}^* \hat{\mathbf{J}}_{k;B}^e + \left(\hat{\mathbf{J}}_{k;A}^e \right)^* \hat{\mathbf{E}}_{k;B} \right] d^3 \mathbf{x} \\ &= \oint_{\mathbf{x} \in \partial \mathbb{D}} \left(\hat{\mathbf{E}}_{j;A}^* L_{jk} \hat{\mathbf{H}}_{k;B} + \hat{\mathbf{E}}_{j;B} L_{jk} \hat{\mathbf{H}}_{k;A}^* \right) d^2 \mathbf{x} \\ & - \int_{\mathbf{x} \in \Sigma_{\text{int}}} \tau_{ij} \hat{\mathbf{E}}_{j;A}^* b_{il}^{(11)} \tau_{lm} \hat{\mathbf{E}}_{m;B} d^2 \mathbf{x} \\ & + \int_{\mathbf{x} \in \Sigma_{\text{int}}} \tau_{ij} \hat{\mathbf{E}}_{j;A}^* b_{il}^{(12)} L_{lm} \hat{\mathbf{H}}_{m;B} d^2 \mathbf{x} \\ & + \int_{\mathbf{x} \in \Sigma_{\text{int}}} L_{ij} \hat{\mathbf{H}}_{j;A}^* b_{il}^{(21)} \tau_{lm} \hat{\mathbf{E}}_{m;B} d^2 \mathbf{x} \\ & - \int_{\mathbf{x} \in \Sigma_{\text{int}}} L_{ij} \hat{\mathbf{H}}_{j;A}^* b_{il}^{(22)} L_{lm} \hat{\mathbf{H}}_{m;B} d^2 \mathbf{x}. \quad (27) \end{aligned}$$

Because the magnetic current sources are taken zero, the magnetic field that is still present in the integrals can be replaced by

$\hat{\mathbf{H}}_j = -\hat{m}_{jp} (\hat{\zeta}_{pq} + (j\omega)^{-1} \epsilon_{pmq} \partial_n) \hat{\mathbf{E}}_q$, where m_{pq} is the inverse of the magnetic permeability tensor, given by $\hat{m}_{pq} \hat{l}_{qr} = \delta_{pr}$. In case the interfaces have impedance boundary conditions that do not dissipate energy all boundary condition tensors vanish, $b_{il}^{(\alpha\beta)} = 0$, and only the integral over the outer boundary remains. In case the interfaces are perfect electric (PEC), or perfect magnetic (PMC) conductors, the integrals vanish because the tangential electric and/or magnetic fields vanish. In those situations the perfect conducting boundary can be taken as part of the outer boundary $\partial \mathbb{S}$, because such interface behaves as a perfect reflector with possible polarization rotation. When small losses occur, e.g., when the conducting boundaries are not perfect, but still good conductors [31], a small error will be introduced when the boundary integrals are ignored, similar to ignoring the volume integral when the background medium is slightly dissipative [30]. Equation (27) is the starting point to formulate the numerical examples. Even when the impedance conditions involve energy dissipation at the interface and sources on the interface are required to retrieve correct Green's functions, no numerical singularities occur, unless a receiver is located at the interface with an impedance condition. In such situations it is not useful to retrieve Green's functions for a source and/or receiver at the impedance boundary, because then the easiest way is direct computation. We are interested in remote sensing without having a source close to the impedance boundary and we will show numerical examples for two different impedance conditions.

VI. EXAMPLES

The most interesting situations occur when the propagating medium is lossless. We will investigate two different types of IBC interfaces in two dimensions. The TE-mode Maxwell's equations for a 2-D bianisotropic medium is written as

$$\begin{pmatrix} 0 & -\partial_3 & \partial_1 \\ -\partial_3 & 0 & 0 \\ \partial_1 & 0 & 0 \end{pmatrix} \begin{pmatrix} \hat{\mathbf{E}}_2 \\ \hat{\mathbf{H}}_1 \\ \hat{\mathbf{H}}_3 \end{pmatrix} + j\omega \begin{pmatrix} \epsilon & \xi_{21} & \xi_{23} \\ \zeta_{12} & \mu & 0 \\ \zeta_{32} & 0 & \mu \end{pmatrix} \begin{pmatrix} \hat{\mathbf{E}}_2 \\ \hat{\mathbf{H}}_1 \\ \hat{\mathbf{H}}_3 \end{pmatrix} = \begin{pmatrix} -\hat{\mathbf{J}}_2^e \\ 0 \\ 0 \end{pmatrix} \quad (28)$$

Correlation reciprocity is used in a bounded 2-D domain \mathbb{S} , with outward unit normal $\mathbf{n} = (n_1, 0, n_3)^T$, in a medium that is adjacent to the medium for which the electric field scalar Green's function is retrieved.

The reciprocity theorem of the time correlation type of (27) reduces to

$$\begin{aligned} & \int_{\mathcal{S}} \left[\left\{ \hat{E}_{2;A}^{(a)} \right\}^* \hat{J}_{2;B}^e + \hat{E}_{2;B}^{(a)} \left\{ \hat{J}_{2;A}^e \right\}^* \right] d^2 \mathbf{x} \\ &= \frac{1}{j\omega} \oint_{\partial \mathcal{S}} \mu^{-1} \left[\left\{ \hat{E}_{2;A}^{(a)} \right\}^* n_m \partial_m \hat{E}_{2;B}^{(a)} - \hat{E}_{2;B}^{(a)} n_m \partial_m \left\{ \hat{E}_{2;A}^{(a)} \right\}^* \right] d\mathbf{x} \\ &+ 2 \oint_{\partial \mathcal{S}} \mu^{-1} \epsilon_{km2} n_k \Re \{ \xi_{2m} \} \left\{ \hat{E}_{2;A}^{(a)} \right\}^* \hat{E}_{2;B}^{(a)} d\mathbf{x} \end{aligned} \quad (29)$$

where it is understood that $n_2 = 0$ in this 2-D example. Equation (29) is the 2-D equivalent of (27) in which the second and third equations from (28) have been used to write the magnetic field in terms of the electric field. This is the diagonalization procedure, mentioned below (19). Notice that we have used the adjoint states for (29), for which reason ξ_{2m} occurs in the third integral instead of ζ_{m2} . As a consequence of eliminating the magnetic field from the equation, it can be seen in (29) that for a lossless nonreciprocal medium, where ξ_{kr} has a nonvanishing real part, an extra integral over the boundary remains in the time-correlation type reciprocity theorem compared to an ordinary anisotropic and reciprocal lossless medium. For a bianisotropic reciprocal lossless medium $\Re \{ \xi_{kr} \} = 0$, and, hence, the second integral on the right-hand side of (29) vanishes. In that case (29) reduces to the same form as for an ordinary anisotropic reciprocal lossless medium.

We take the medium parameters in the two states A and B the same and that of the medium adjoint to the actual medium; the electric current source in state A to be a line source given by $\hat{J}_{2;A}^e = \delta(x_1 - x_{1;A})\delta(x_3 - x_{3;A})$ and a similar choice for $J_{2;B}^e$. The electric field can be written in terms of the Green's function as $\hat{E}_2^{(a)}(\mathbf{x}, \omega) = \hat{G}^{(a)}(\mathbf{x}, \mathbf{x}', \omega)$ and is substituted in (29) to obtain

$$\begin{aligned} & \left\{ \hat{G}^{(a)}(\mathbf{x}_B, \mathbf{x}_A, \omega) \right\}^* + \hat{G}^{(a)}(\mathbf{x}_A, \mathbf{x}_B, \omega) \\ &= \frac{1}{j\omega\mu} \oint_{\partial \mathcal{S}} \left\{ \hat{G}^{(a)}(\mathbf{x}, \mathbf{x}_A, \omega) \right\}^* n_m \partial_m \hat{G}^{(a)}(\mathbf{x}, \mathbf{x}_B, \omega) d\mathbf{x} \\ &- \frac{1}{j\omega\mu} \oint_{\partial \mathcal{S}} \hat{G}^{(a)}(\mathbf{x}, \mathbf{x}_B, \omega) n_m \partial_m \left\{ \hat{G}^{(a)}(\mathbf{x}, \mathbf{x}_A, \omega) \right\}^* d\mathbf{x} \\ &+ \frac{2}{\mu} \oint_{\partial \mathcal{S}} W(\mathbf{x}, \omega) \left\{ \hat{G}^{(a)}(\mathbf{x}, \mathbf{x}_A, \omega) \right\}^* \hat{G}^{(a)}(\mathbf{x}, \mathbf{x}_B, \omega) d\mathbf{x} \end{aligned} \quad (30)$$

where $W(\mathbf{x}, \omega) = \epsilon_{km2} n_k \Re \{ \xi_{2m} \}$. Exploiting the fact that $\hat{G}^{(a)}(\mathbf{x}', \mathbf{x}, \omega) = \hat{G}(\mathbf{x}, \mathbf{x}', \omega)$ all the Green's functions in (30) belonging to the adjoint medium are replaced with the Green's function in the actual medium and (30) is rewritten as

$$\begin{aligned} & \hat{G}^*(\mathbf{x}_A, \mathbf{x}_B, \omega) + \hat{G}(\mathbf{x}_B, \mathbf{x}_A, \omega) \\ &= \frac{1}{j\omega\mu} \oint_{\partial \mathcal{S}} \hat{G}^*(\mathbf{x}_A, \mathbf{x}, \omega) n_m \partial_m \hat{G}(\mathbf{x}_B, \mathbf{x}, \omega) d\mathbf{x} \\ &- \frac{1}{j\omega\mu} \oint_{\partial \mathcal{S}} \hat{G}(\mathbf{x}_B, \mathbf{x}, \omega) n_m \partial_m \hat{G}^*(\mathbf{x}_A, \mathbf{x}, \omega) d\mathbf{x} \\ &+ \frac{2}{\mu} \oint_{\partial \mathcal{S}} W(\mathbf{x}, \omega) \hat{G}^*(\mathbf{x}_A, \mathbf{x}, \omega) \hat{G}(\mathbf{x}_B, \mathbf{x}, \omega) d\mathbf{x}. \end{aligned} \quad (31)$$

Equation (31) is the Green's function extraction relation for the 2-D electric field in a lossless bianisotropic medium with interfaces satisfying general lossless or perfect conducting impedance boundary conditions.

In the high-frequency approximation, where $n_m \partial_m \hat{G}(\mathbf{x}_A, \mathbf{x}, \omega) \approx -(\epsilon_{km2} n_k \xi_{2m} + \sqrt{\epsilon\mu}) j\omega \hat{G}(\mathbf{x}_A, \mathbf{x}, \omega)$, the first integral in the right-hand side of (31) becomes equal to the second integral with opposite sign, while the third integral is approximately cancelled, such that only the term with $j\omega\sqrt{\epsilon\mu}$ remains and we use $c = 1/\sqrt{\epsilon\mu}$ as the wave propagation velocity ignoring the bianisotropy effects. Under these approximations (31) reduces to

$$\begin{aligned} & \hat{G}^*(\mathbf{x}_A, \mathbf{x}_B, \omega) + \hat{G}(\mathbf{x}_B, \mathbf{x}_A, \omega) \\ &\approx -\frac{2}{\mu c} \oint_{\partial \mathcal{S}} \hat{G}^*(\mathbf{x}_A, \mathbf{x}, \omega) \hat{G}(\mathbf{x}_B, \mathbf{x}, \omega) d\mathbf{x} \end{aligned} \quad (32)$$

which is the desired relation to extract the Green's function between \mathbf{x}_A and \mathbf{x}_B from the product of the complex conjugate of the Green's function between a receiver in \mathbf{x}_A and sources on the boundary $\partial \mathcal{S}$ and the Green's function between a receiver in \mathbf{x}_B and sources on the boundary $\partial \mathcal{S}$. The effect of making these approximations are investigated by comparing results from (31) and (32).

A. Lossless and PEC Impedance Boundaries

For the numerical examples it suffices to investigate a simple 2-D configuration. We choose a homogeneous bianisotropic background medium in which one planar boundary occurs that satisfies an impedance boundary condition, located at $x_3 = 0$. We place two outer boundaries such that $\partial \mathcal{S} = \partial \mathcal{S}_1 + \partial \mathcal{S}_2$, with $\partial \mathcal{S}_1$ is defined by $x_{3;1} = -8$ m and $\partial \mathcal{S}_2$ is defined by $x_{3;2} = 5$ m. The points \mathbf{x}_A and \mathbf{x}_B are located at the depth level $x_{3;A} = -2$ m and $x_{3;B} = -1$ m and $x_{1;B} - x_{1;A} = -1$ m. The medium parameters are given by $\epsilon = 9\epsilon_0$, $\mu = \mu_0$, $\xi_{21} = \zeta_{12} = 5 \times 10^{-9}$ and $\xi_{23} = \zeta_{32} = 1 \times 10^{-9}$. For this choice of bianisotropy parameters $Wc = 0.5$ on the boundaries $\partial \mathcal{S}_1$ and $\partial \mathcal{S}_2$, where W is given below (30) and c is defined just above (32). The actual propagating wave velocity in the positive x_3 -direction is $c_3^+ = 203$ mm/ns, in the negative x_3 -direction it is $c_3^- = 67$ mm/ns, while in the positive and negative x_1 -directions they are $c_1^+ = 124$ mm/ns and $c_1^- = 164$ mm/ns. The boundary parameters are given by $\epsilon^b = \epsilon_0/10$, $\mu^b = \mu_0/20$, $\xi^b = \zeta^b = 5 \times 10^{-10}$. We use the second derivative of a Gaussian as the source pulse, with a central frequency of 250 MHz as spectral bandwidth filter; we place 1024 electric dipoles separated by 5 cm on $\partial \mathcal{S}_1$ and $\partial \mathcal{S}_2$. Because we model propagating waves, the usual discretization conditions apply to avoid spatial and temporal aliasing. We show results for a horizontal distance of 1 m between the two receivers. The result from summing the correlated signals received at \mathbf{x}_A and \mathbf{x}_B from sources at both interfaces according to (31) is shown in Fig. 3(a), according to (31) but ignoring the third integral on the left-hand side, and according to (32) in Fig. 3(c). The left-hand sides of (31) and (32) can be computed as exact results in the time-domain and these are shown in solid black lines for a source in \mathbf{x}_A and a receiver in \mathbf{x}_B for positive times and for a source \mathbf{x}_B and a receiver in \mathbf{x}_A for

negative times. The right-hand sides of (31) and (32) describe how the retrieved results should be obtained and the numerical results are shown in red dashed lines. The finite length of the source boundaries leads to break-off errors that can be seen in the direct waves that travel between source and receiver in all the plots in Fig. 3. Still the retrieved signal is quite accurate in amplitude and perfect in time. The reflection event is very accurately retrieved, because the sources that are stationary for this reflection event are relatively close to the receivers. To investigate the contribution from the third integral in the right-hand side of (31) we plot the result of the first two integrals in the right-hand side of (31) in Fig. 3(b), where the direct wave in positive times has a much too low amplitude, the direct wave at negative times has a much too high amplitude, while the reflected waves, at both positive and negative times, from the impedance boundary have approximately half the expected amplitude. Implementing the high-frequency approximation is expected to give larger errors in the direct waves than in the reflected events, because in the approximation it is assumed that the wave field that contributes to the retrieved events, leaves the source boundary perpendicular to this boundary. For receivers at an angle of 45 degrees with the vertical axis the waves that are stationary for retrieving the direct field leave the boundary at 45 degrees and we expect an error in the amplitude of $1/\cos(\pi/4) = \sqrt{2}$ as can be seen in Fig. 3(c), where it can also be seen that the reflection from the impedance boundary has no visible error. The asymmetry in the amplitudes of the retrieved direct waves at positive and negative times is because the propagating medium is bianisotropic.

In Fig. 4 similar results are shown for a PEC boundary. For a PEC boundary the sources are only necessary on boundary $\partial\mathcal{S}_1$, because the boundary $\partial\mathcal{S}_2$ lies below the PEC boundary, which is a perfect reflector and waves sent from sources on the boundary $\partial\mathcal{S}_2$ do not reach the points \mathbf{x}_A and \mathbf{x}_B . The retrieved result using (31) is excellent (Fig. 4(a)), and the PEC reflection retrieved from (32) is very good with a slight amplitude error (Fig. 4(b)). The direct events at negative times are now also retrieved from sources on $\partial\mathcal{S}_1$ and this leads to interactions of waves that leave the boundary in positive x_3 -direction, reflect off the PEC boundary, traveling in negative x_3 -direction, and pass through both receivers in \mathbf{x}_B and then \mathbf{x}_A . These interactions are different than in the example with nonperfect reflecting impedance boundary where the direct waves at positive times are retrieved from sources on $\partial\mathcal{S}_2$. For this reason the direct events at positive times in Fig. 4(a) and (b) are slightly different from the direct events at positive times in Fig. 3(a) and (c), respectively.

VII. CONCLUSION

The matrix representation for Green's function retrieval in general bianisotropic media with IBC interfaces holds for non-reciprocal and dissipative media. It applies to natural and engineered media. The validity of the Green's function retrieval by cross correlation of two noise field recordings has been extended to include media with interfaces that are characterized by jump-average conditions. The condition of the media and IBC interfaces being lossless was shown to be a sufficient condition to create new data from measured data due to noise sources on

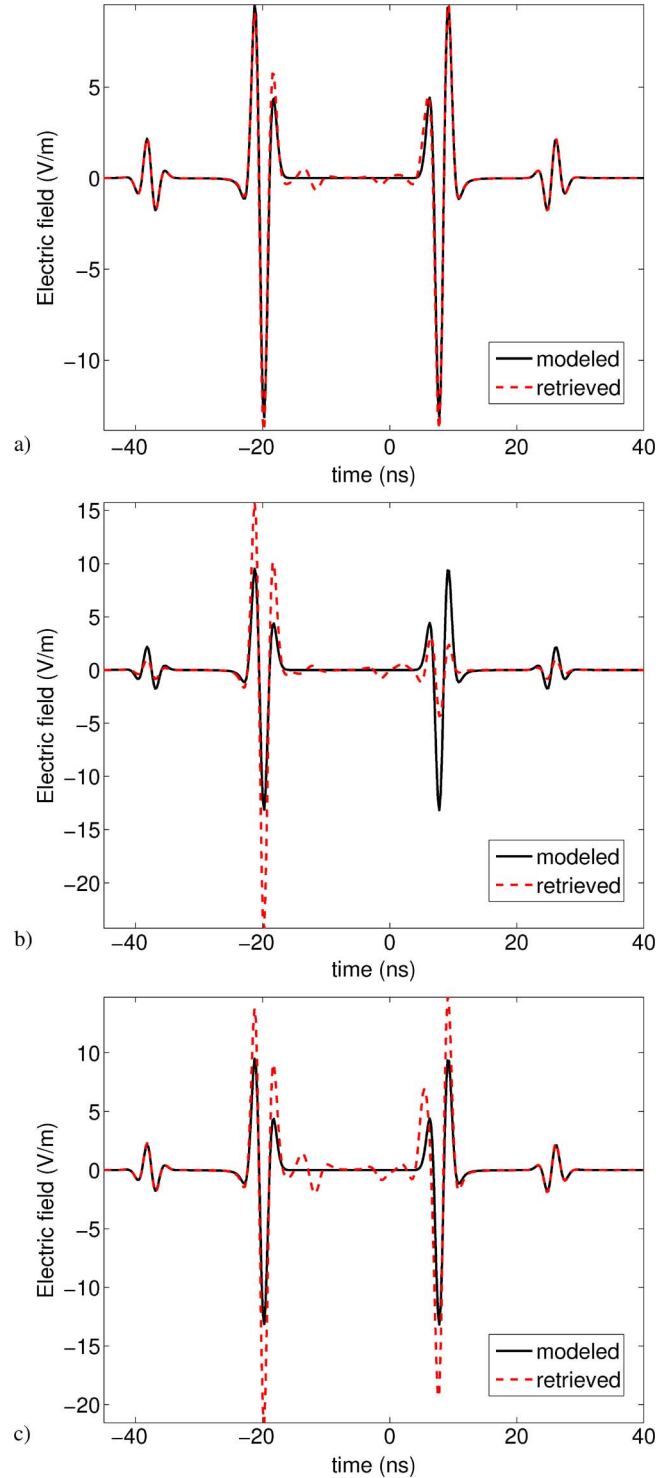


Fig. 3. Exact results for a boundary satisfying lossless bianisotropic boundary conditions in a bianisotropic medium are shown in solid black lines for a source in \mathbf{x}_A and a receiver in \mathbf{x}_B for positive times and for a source \mathbf{x}_B and a receiver in \mathbf{x}_A for negative times, which is equal to the time-domain equivalent of the left-hand sides of equations (31) and (32); retrieved results are shown in red dashed lines, which are obtained according to the right-hand side of a) equation (31), b) same as a) but ignoring the third integral, and c) (32).

a remote closed boundary only. The result may find applications in a wide variety of fields, ranging from microwave to optical regimes, and the most interesting application is to obtain pulse-echo data from cross correlations of noise observations

ACKNOWLEDGMENT

This work is part of the research program of the Netherlands research center for Integrated Solid Earth Science (ISES).

REFERENCES

- [1] E. Slob and K. Wapenaar, "Electromagnetic Green's functions retrieval by cross-correlation and cross-convolution in media with losses," *Geophys. Res. Lett.*, vol. 34, no. 5, p. L05307, 2007.
- [2] L. B. Liu and K. He, "Wave interferometry applied to borehole radar: Virtual multioffset reflection monitoring," *IEEE Trans. Geosci. Remote Sens.*, vol. 45, no. 8, pp. 2554–2559, Aug. 2007.
- [3] E. Slob and K. Wapenaar, "GPR without a source: Cross-correlation and cross-convolution methods," *IEEE Trans. Geosci. Remote Sens.*, vol. 45, no. 8, pp. 2501–2510, Aug. 2007.
- [4] E. Slob and K. Wapenaar, "Practical representations of electromagnetic interferometry for GPR applications: A tutorial," *Near Surface Geophys.*, vol. 6, no. 6, pp. 391–402, Dec. 2008.
- [5] E. Slob, "Interferometry by deconvolution of multi-component multioffset GPR data," *IEEE Trans. Geosci. Remote Sens.*, vol. 47, no. 3, pp. 828–838, Mar. 2009.
- [6] A. Kaufman and G. Keller, "Frequency and transient soundings," in *Methods Geochem. Geophys.*. New York: Elsevier, 1983, vol. 16.
- [7] Z. G. Qian, W. C. Chew, and R. Suaya, "Generalized impedance boundary condition for conductor modeling in surface integral equation," *IEEE Trans. Microw. Theory Tech.*, vol. 55, no. 11, pp. 2354–2364, Nov. 2007.
- [8] O. Özdemir, I. Akduman, A. Yapar, and L. Crocco, "Higher order inhomogeneous impedance boundary conditions for perfectly conducting objects," *IEEE Trans. Geosci. Remote Sens.*, vol. 45, no. 5, pt. 1, pp. 1291–1297, May 2007.
- [9] I. Hänninen and K. Nikoskinen, "Implementation of method of moments for numerical analysis of corrugated surfaces with impedance boundary condition," *IEEE Trans. Antennas Propagat.*, vol. 56, no. 1, pp. 278–281, Jan. 2008.
- [10] M. F. Catedra, C. Delgado, and I. G. Diego, "New physical optics approach for an efficient treatment of multiple bounces in curved bodies defined by an impedance boundary condition," *IEEE Trans. Antennas Propagat.*, vol. 56, no. 3, pp. 728–736, Mar. 2008.
- [11] J. Komijani and J. Rashed-Mohassel, "Symmetrical properties of dyadic Green's functions for mixed boundary conditions and integral representations of the electric fields for problems involving a PEMC," *IEEE Trans. Antennas Propagat.*, vol. 57, no. 10, pt. Part 2, pp. 3199–3204, Oct. 2009.
- [12] S. Yuferev and L. Di Rienzo, "Surface impedance boundary conditions in terms of various formalisms," *IEEE Trans. Magn.*, vol. 46, no. 9, pp. 3617–3628, Sep. 2010.
- [13] P. Yla-Oijala, S. P. Kiminki, and S. Jarvenpaa, "Solving IBC-CFIE with dual basis functions," *IEEE Trans. Antennas Propagat.*, vol. 58, no. 12, pp. 3997–4004, Dec. 2010.
- [14] Y. Z. Umul and U. Yalcin, "The effect of impedance boundary conditions on the potential function of the boundary diffraction wave theory," *Opt. Commun.*, vol. 281, no. 1, pp. 23–27, Jan. 2008.
- [15] R. B. Clipp and B. N. Steele, "Impedance boundary conditions for the pulmonary vasculature including the effects of geometry, compliance, and respiration," *IEEE Trans. Biomed. Eng.*, vol. 56, no. 3, pp. 862–870, Mar. 2009.
- [16] D. Khaliullin and S. Tret'yakov, "Generalized impedance-type boundary conditions for thin planar layers of various media (review)," *J. Commun. Technol. Electron.*, vol. 43, no. 1, pp. 12–25, Jan 1998.
- [17] V. Galdi and I. M. Pinto, "Derivation of higher-order impedance boundary conditions for stratified coatings composed of inhomogeneous-dielectric and homogeneous-bianisotropic layers," *Radio Sci.*, vol. 35, pp. 287–303, 2000.
- [18] J. Kong, "Theorems of bianisotropic media," *Proc. IEEE*, vol. 60, no. 9, pp. 1036–1046, Sep. 1972.
- [19] W. W. Chow, J. Gea-Banacloche, L. M. Pedrotti, V. E. Sanders, W. Schleich, and M. O. Scully, "The ring laser gyro," *Rev. Modern Phys.*, vol. 57, no. 1, pp. 61–104, Jan. 1985.
- [20] E. Slob and K. Wapenaar, "Retrieving the Green's function from cross correlation in a bianisotropic medium," *Progr. Electromagn. Res.-PIER*, vol. 93, pp. 255–274, 2009.

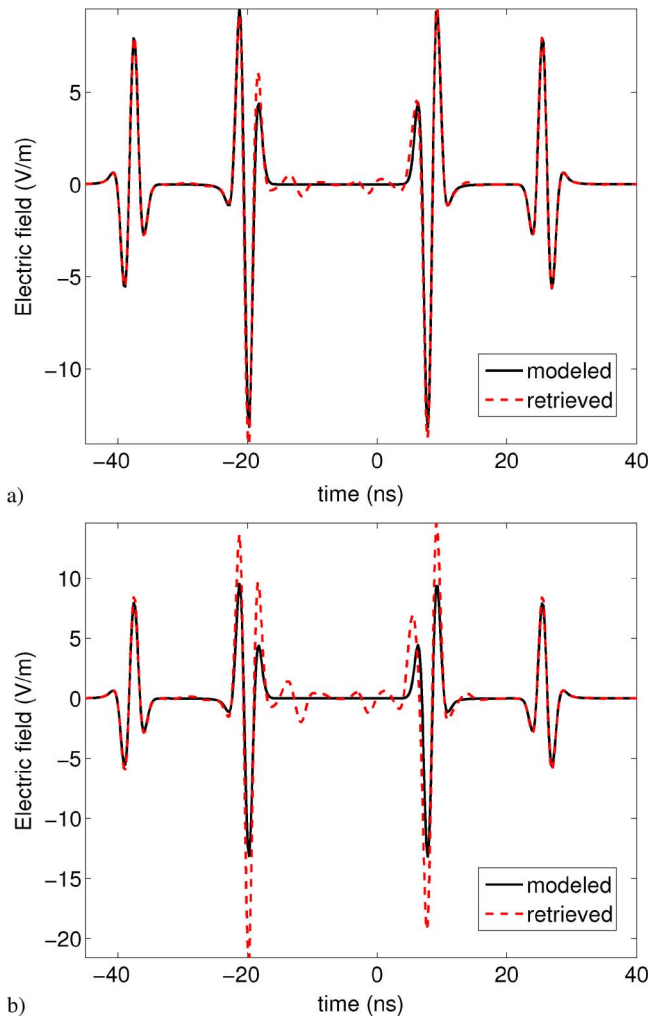


Fig. 4. Exact results for a boundary satisfying PEC boundary conditions in a bianisotropic medium are shown in solid black lines for a source in \mathbf{x}_A and a receiver in \mathbf{x}_B for positive times and for a source \mathbf{x}_B and a receiver in \mathbf{x}_A for negative times, which is equal to the time-domain equivalent of the left-hand sides of equations (31) and (32); retrieved results are shown in red dashed lines, which are obtained according to the right-hand sides of equations (31) and (32).

for imaging and characterization of natural and engineered materials.

We derived electric field Green's function extraction from summing correlations of field recordings from sources on a boundary. In the following 2-D numerical examples we have shown that the high-frequency approximation provides reasonably accurate results for reflection events from lossless impedance interfaces as well as PEC boundaries. When the source array has a wide enough aperture, direct waves are well reconstructed even when the line between the two receivers is parallel to the source planes. In configurations where the bianisotropy parameters lead to an extra integral over the source boundary, the high-frequency approximation leads to kinematically correct direct waves and dynamically accurate reconstruction of reflection events. This still applies when the bianisotropy parameters cannot be considered small and without needing to know the bianisotropy parameters.

- [21] A. Sihvola, "Metamaterials in electromagnetics," *Metamaterials*, vol. 1, no. 1, pp. 2–11, 2007.
- [22] I. Lindell and A. Sihvola, "Generalized soft-and-hard surface," *IEEE Trans. Antennas Propagat.*, vol. 50, no. 7, pp. 926–929, Jul. 2002.
- [23] I. Lindell and A. Sihvola, "Realization of the PEMC boundary," *IEEE Trans. Antennas Propagat.*, vol. 53, no. 9, pp. 3012–3018, Sep. 2005.
- [24] I. Lindell, A. Sihvola, and K. Suchy, "Six-vector formalism in electromagnetics of bi-anisotropic media," *J. Electromagn. Waves Appl.*, vol. 9, no. 7–8, pp. 887–903, 1995.
- [25] K. Wapenaar, E. Slob, and J. Fokkema, "Reciprocity and power balance for piecewise continuous media with imperfect interfaces," *J. Geophys. Res. B*, vol. 109, no. 10, p. B10301, 2004.
- [26] D. Hoppe and Y. Rahmat-Samii, *Impedance Boundary Conditions in Electromagnetics*. Bristol, PA: Taylor and Francis, 1995.
- [27] V. Rumsey, "Reaction concept in electromagnetic theory," *Phys. Rev.*, vol. 94, pp. 1483–1491, 1954.
- [28] K. Wapenaar, E. Slob, and R. Snieder, "Unified Green's function retrieval by cross correlation," *Phys. Rev. Lett.*, vol. 97, no. 23, pp. 234301-1–234301-4, 2006.
- [29] K. Wapenaar, "General wave field representations for seismic modeling and inversion," *Geophysics*, vol. 72, no. 5, pp. SM5–SM17, 2007.
- [30] E. Slob, D. Draganov, and K. Wapenaar, "Interferometric electromagnetic Green's functions representations using propagation invariants," *Geophys. J. Int.*, vol. 169, no. 1, pp. 60–80, 2007.
- [31] I. V. Lindell and A. H. Sihvola, "Losses in the PEMC boundary," *IEEE Trans. Antennas Propagat.*, vol. 54, no. 9, pp. 2553–2558, Sep. 2006.

Evert Slob, photograph and biography not available at the time of publication.

Kees Wapenaar, photograph and biography not available at the time of publication.